Effects of pressure on structural, electronic, and mechanical properties of α, β, and γ uranium*

Hui-Jie Zhang(张慧杰)[1], Shi-Na Li(李世娜)[1], Jing-Jing Zheng(郑晶晶)[1], Wei-Dong Li(李卫东)[1], and Bao-Tian Wang(王保田)[2,3,†]

[1] *Institute of Theoretical Physics and Department of Physics, Shanxi University, Taiyuan* 030006, *China*
[2] *Institute of High Energy Physics, Chinese Academy of Sciences (CAS), Beijing* 100049, *China*
[3] *Dongguan Neutron Science Center, Dongguan* 523803, *China*

(Received 6 December 2016; revised manuscript received 9 March 2017; published online 10 May 2017)

The first-principles methods have been employed to calculate the structural, electronic, and mechanical properties of the α, β, and γ phases of uranium under pressure up to 100 GPa. The electronic structure has been viewed in forms of density of states and band structure. The mechanical stability of metal U in the α, β, and γ phases have been examined. The independent elastic constants, polycrystalline elastic moduli, as well as Poisson's ratio have been obtained. Upon compression, the elastic constants, elastic moduli, elastic wave velocities, and Debye temperature of α phase are enhanced pronouncedly. The value of B/G illustrates that α and γ phases are brittle in ground state.

Keywords: first-principles, structural parameters, electronic structure, elastic constants

PACS: 61.50.Ah, 61.50.Ks, 71.20.–b, 62.20.–x **DOI:** 10.1088/1674-1056/26/6/066104

1. Introduction

Actinide elements and their compounds exhibit many fascinating physical behaviors and play special role in nuclear applications,[1–8] for example, the superconductivity of the f-electron system,[9] the complex magnetic structure in neptunium dioxide,[10] and the topological electronic states in actinide nitrides.[11] Among them, element uranium has attracted many attentions.[12–18]

At ambient condition, the itinerant nature of U-5f electrons results in a complex arrangement of atomic structure,[12–15] a low symmetrical crystal structure of face-centered orthohombic (fco). This phase, α-U, is stable in wide temperature range of 0 K–935 K and wide pressure area up to at least 100 GPa. At ambient pressure and under a narrow temperature range of 935 K–1045 K, a much complex β phase appears.[13,19] Under further high temperature of 1045 K–1460 K, in analogy to the transition metals of Ti, Zr, and Hf,[20,21] β-U transits to a simple high-symmetry structure of body-centered cubic (bcc). The driving mechanism for this kind of transition has been attributed to the electron localization[22] and/or the phonon-phonon interaction.[23]

Concerning the physical properties, in experiments, the charge density wave (CDW) state below 43 K,[24] bulk modulus and equation of state,[12–15] phase diagram at high pressure and temperature,[13] phonon-dispersion carves,[25,26] and heat capacity[27] of uranium were measured by ultrasonic technique, diamond anvil cell, x-ray diffraction, inelastic neutron scattering. In theory, the adiabatic compression curve up to 100 GPa,[16] effects of spin-orbit coupling,[17] mechanical properties,[18,28,29] melting,[30] optical properties,[31] work function,[32] and phonon spectra,[18,23,33] CDW,[34–36] and electron–phonon coupling[35] have been calculated in density-functional theory (DFT) level.

In this work, we use the first-principles DFT to carry out studies on the structural, electronic, and mechanical properties of uranium in its α, β, and γ phases under pressure up to 100 GPa. Specific details can be divided into four parts: (i) optimizing all lattice parameters and the internal degrees of freedom at selected volumes and then at our obtained pressures; (ii) comparing the enthalpy of the three phases to see the thermodynamic stability under pressure; (iii) analyzing the electronic structure; and (iv) calculating elastic constants and elastic moduli under different pressures.

2. Computational methods

We performed our first-principles DFT calculations within the Vienna *ab initio* simulation package (VASP).[37] The Perdew–Burke–Ernzerhof[38] form of the generalized gradient approximation was selected to described the exchange and correlation effects. A cutoff energy of 500 eV was set for the plane wave integration. All atoms were fully relaxed when Hellmann–Feynman forces become less than 0.01 eV/Å. The k-point meshes in the full wedge of the Brillouin zone (BZ) were sampled by 11×7×7, 7×7×13, and 13×13×13 grids, respectively for α, β, and γ phases according to the Monkhorst–Pack (MP)[39] scheme. The U $6s^2 7s^2 6p^6 6d^2 5f^2$

*Project supported by the National Natural Science Foundation of China (Grant No. 11374197).
†Corresponding author. E-mail: wangbt@ihep.ac.cn
© 2017 Chinese Physical Society and IOP Publishing Ltd

orbitals were treated as valence electrons.

To avoid the Pulay stress trouble, the geometry optimization was performed on the basis of fixed volumes rather than constant pressures. As shown in Fig. 1, we calculated the total energy versus volume data for the three phases in the first-step, then performed the seventh-order polynomial fitting and obtained the E–V relation. Then, one can deduce the P–V relation by the thermodynamic derivative $P=-\partial E/\partial V$. Using this P–V relation, we performed the second-step calculations at a series of volumes correspinding to some integer pressures. Note that these pressure values are different from the pressure values directly computed from DFT with the Hellmann–Feynman theorem.

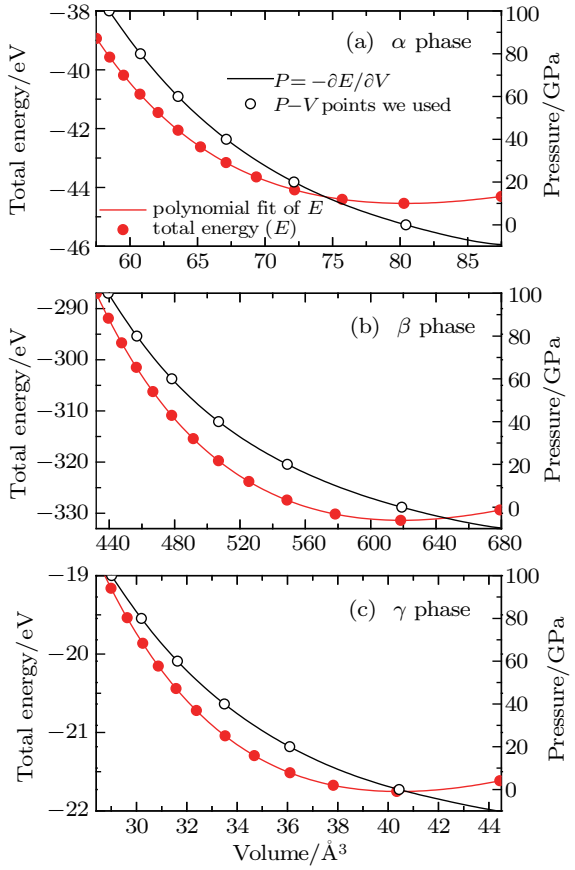


Fig. 1. (color online) The total energy (E)–volume (V) and the pressure (P)–V relations of α, β, and γ phases. The red solid circles are the first-step calculated E. Then we do polynomial fitting to these data and obtain the solid red line. Using the polynomial fitted E–V, we can deduce the P by the relation $P=-\partial E/\partial V$. The integrated values of P, used in the following calculations, are indicated by the black hollow circles.

In order to calculate elastic constants, we can apply stress tensors with a small strain onto the equilibrium structure. According to Hooke's law, the crystal energy is expanded by Taylor,[40]

$$E(V,\varepsilon) = E(V_0,0)+V_0\sum_{i=1}^{6}\sigma_i e_i + \frac{V_0}{2}\sum_{i,j=1}^{6}C_{ij}e_ie_j + O\left(\{e_i^3\}\right), \quad (1)$$

where $E(V_0,0)$ is the energy of the unstrained system with the equilibrium volume V_0, ε is strain tensor which has matrix elements ε_{ij} ($i,j=1,2$, and 3) defined by

$$\varepsilon_{ij}=\begin{pmatrix} e_1 & \frac{1}{2}e_6 & \frac{1}{2}e_5 \\ \frac{1}{2}e_6 & e_2 & \frac{1}{2}e_4 \\ \frac{1}{2}e_5 & \frac{1}{2}e_4 & e_3 \end{pmatrix} \quad (2)$$

and C_{ij} are the elastic constants. For orthorhombic α phase, there are nine independent elastic constants (C_{11}, C_{22}, C_{33}, C_{44}, C_{55}, C_{66} C_{12}, C_{13}, and C_{23}). They can be achieved from nine different strains listed in the following:

$$\begin{aligned} \varepsilon_1 &= (\delta,0,0,0,0,0), \quad \varepsilon_2=(0,\delta,0,0,0,0), \\ \varepsilon_3 &= (0,0,\delta,0,0,0), \quad \varepsilon_4=(0,0,0,\delta,0,0), \\ \varepsilon_5 &= (0,0,0,0,\delta,0), \quad \varepsilon_6=(0,0,0,0,0,\delta), \\ \varepsilon_7 &= (\delta,\delta,0,0,0,0), \quad \varepsilon_8=(\delta,0,\delta,0,0,0), \\ \varepsilon_9 &= (0,\delta,\delta,0,0,0). \end{aligned} \quad (3)$$

As for tetragonal β phase, there are six independent elastic constants (C_{11}, C_{33}, C_{44}, C_{66} C_{12}, and C_{13}) and can be obtained from six different strains listed in the following:

$$\begin{aligned} \varepsilon_1 &= (\delta,\delta,\delta,0,0,0), \quad \varepsilon_2=(0,0,0,\delta,\delta,0), \\ \varepsilon_3 &= (\delta,\delta,0,0,0,0), \quad \varepsilon_4=(0,0,0,0,0,\delta), \\ \varepsilon_5 &= (\delta,0,\delta,0,0,0), \quad \varepsilon_6=(0,0,\delta,0,0,0). \end{aligned} \quad (4)$$

For cubic γ phase, there are three independent elastic constants (C_{11}, C_{44}, and C_{12}) and can be gained from three different strains listed in the following:

$$\begin{aligned} \varepsilon_1 &= (\delta,\delta,\delta,0,0,0), \quad \varepsilon_2=(0,0,0,\delta,\delta,\delta), \\ \varepsilon_3 &= (\delta,0,\delta,0,0,0), \end{aligned} \quad (5)$$

where the small strain δ was varied in steps of 0.006 from $\delta=-0.036$ to $\delta=0.036$.

After having obtained the elastic constants, the polycrystalline bulk modulus B and shear modulus G were calculated from the Voigt–Reuss–Hill (VRH) approximations,[41–43] $B=\frac{1}{2}(B_{\rm R}+B_V)$ and $G=\frac{1}{2}(G_{\rm R}+G_V)$. The Young's modulus E and Poisson's ratio ν were calculated through $E=9BG/(3B+G)$ and $\nu=(3B-2G)/[2(3B+G)]$. In the calculation of the Debye temperature ($\theta_{\rm D}$), we used the relation

$$\theta_{\rm D}=\frac{h}{k_{\rm B}}\left(\frac{3n}{4\pi\Omega}\right)^{1/3}\upsilon_{\rm m}, \quad (6)$$

where h and $k_{\rm B}$ are Planck and Boltzmann constants, respectively, n is the number of atoms in the molecule, Ω is molecular volume, and $\upsilon_{\rm m}$ is the average sound wave velocity. The

average wave velocity in the polycrystalline materials is approximately given by

$$\upsilon_{\mathrm{m}} = \left[\frac{1}{3}\left(\frac{2}{\upsilon_{\mathrm{t}}^3} + \frac{1}{\upsilon_{\mathrm{l}}^3}\right)\right]^{-1/3}, \tag{7}$$

in the above expression, $\upsilon_{\mathrm{t}} = \sqrt{G/\rho}$ (ρ is the density) and $\upsilon_{\mathrm{l}} = \sqrt{(3B+4G)/3\rho}$ are the transverse and longitudinal elastic wave velocity of the polycrystalline materials, respectively.

3. Results and discussion

3.1. Atomic structures and lattice parameters

α-U crystallizes in the orthorhombic *Cmcm* space group (No. 63) with 4 atoms in the unit cell located at 4*c* (0, *y*, 0.25) Wyckoff positions [see Fig. 2(a)]. β-U crystallizes in the tetragonal *Pnma* space group (No. 136) with 30 atoms in the unit cell sited at 2*b* (0, 0, 0.5), 4*f* (*x*, *x*, 0), 8*j* (*x*, *x*, *z*), 8*i* (x_1, y_1, 0), and 8*i* (x_2, y_2, 0) Wyckoff positions [see Fig. 2(b)]. γ-U crystallizes in the simple bcc structure [see Fig. 2(c)].

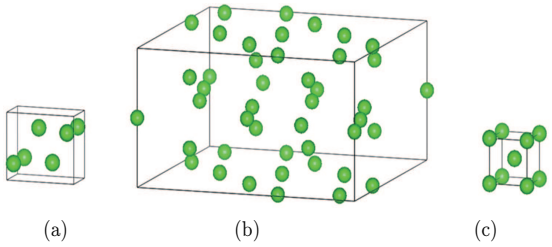


Fig. 2. (color online) Crystal structures of (a) α, (b) β, and (c) γ phases.

In Table 1, we list the lattice parameters, the fractional coordinate of the atoms, atomic volume, bulk modulus and its pressure derivative for α, β, and γ phases at selected pressures in the pressure range of 0 GPa–100 GPa. For three considered phases of uranium, our optimized lattice constants and the atomic volume are well consistent with the recent DFT-PBE data,[29] but slightly lower than the experimental values at 50 K for α-U,[27] at 955 K for β-U,[19] and at 298 K for γ-U.[44] Our calculated bulk moduli are overestimated with respect to the experimental values,[12,13] but close to the DFT-PBE results.[29]

Table 1. Optimized lattice constants (*a*, *b*, and *c*), the fractional coordinate of the atoms (*y*), atomic volume (*V*) under pressures from 0 GPa to 100 GPa as well as bulk modulus (*B*) and its pressure derivative (*B*′) at 0 GPa for α, β, and γ phases of uranium. For comparison, experimental values and theoretical results from other calculations at 0 GPa are also listed.

Phase	Method	Pressure/GPa	*a*/Å	*b*/Å	*c*/Å	*y*	*V*/(Å^3/atom)	*B*/GPa	*B*′
α	this work	0	2.809	5.844	4.898	0.098	20.101	142.2	5.0
		20	2.692	5.600	4.782	0.099	18.023		
		40	2.625	5.423	4.716	0.100	16.784		
		60	2.578	5.290	4.662	0.101	15.895		
		80	2.541	5.173	4.624	0.102	15.195		
		100	2.510	5.085	4.579	0.102	14.611		
	Expt.	0	2.836[27]	5.867[27]	4.936[27]	0.102[27]	20.535[27]	125[12]	6.2[12]
	DFT-PBE[29]	0	2.793	5.849	4.894	0.098	19.987	151	
β	this work	0	10.464		5.653		20.633	126.8	4.8
		20	10.110		5.372		18.303		
		40	9.880		5.193		16.897		
		60	9.699		5.085		15.945		
		80	9.551		5.009		15.310		
		100	9.425		4.946		14.645		
	Expt.[19]	0	10.759		5.635		21.812		
	DFT-PBE[29]	0	10.454		5.634		20.524	130	
γ	this work	0	3.432				20.212	133.6	4.9
		20	3.305				18.051		
		40	3.223				16.740		
		60	3.163				15.822		
		80	3.114				15.098		
		100	3.073				14.510		
	Expt.	0	3.47[44]				20.89[44]	113.3[13]	3.37[13]
	DFT-PBE[29]	0	3.427				20.124	132	

The thermodynamic stabilities of α, β, and γ phases under pressure up to 100 GPa can be judged by comparing the Gibbs free energy values. At 0 K, the the Gibbs free energy is equal to the enthalpy and can be obtained by $G = H = E + PV$. We plot in Fig. 3 the relative enthalpies of the α and γ phases with respect to the β phase as a function of pressure. In the whole pressure range, there are no crossing points for the three curves. The α phase is always thermodynamically stable up to 100 GPa. The pressure can reduce the ΔH between the γ and β phases, while increase the ΔH between the α and β phases. As shown in Fig. 3, the curves of the relative enthalpies of the α and γ phases with respect to the β phase are almost parallel, which shows that the effect of pressure on the ΔH between the γ and α phases is neglectful. These facts are in good agree-

ment with experiments.[13,15] Here, one may wish to stabilize the simple bcc structure at ambient conditions. However, according to our simulations as well as previous experiments, the bcc phase can only be stabilized by increasing temperature, at least in pressure range of 0 GPa–100 GPa.

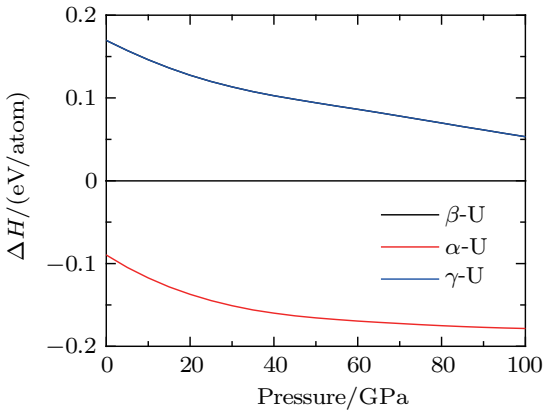


Fig. 3. (color online) Calculated enthalpy differences of the α and the γ phases with respect to the β phase as a function of pressure.

3.2. Electronic properties

In order to study the effects of pressure on electronic structure, the total and partial density of states (DOSs) of α, β, and γ uranium at 0, 40, 100 GPa are plotted in Fig. 4. Near the Fermi level, the main contribution is from the $5f$ and $6d$ orbitals. The occupations of the $5f$ orbitals at the Fermi level for α-U and γ-U decrease evidently under pressure. Even so, the main occupation near the Fermi level is still from the $5f$ orbitals which should play a key role in many macroscopical properties, for example, the hardness, elasticity, and conductivity. For β-U, the occupations of the $5f$ orbitals at the Fermi level behaves in an oscillation way under pressure. Since the β phase only appears in a narrow pressure range in the P–T phase diagram,[13] we will focus our sight on the pressure effects on the α and γ phases.

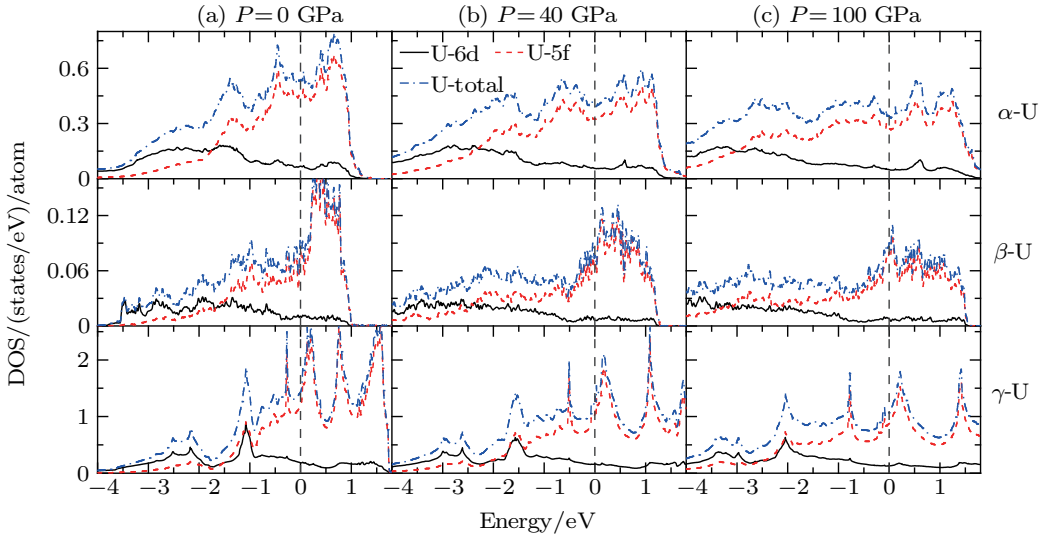


Fig. 4. (color online) Total and partial densities of states for α, β, and γ phases of uranium at (a) 0 GPa, (b) 40 GPa, and (c) 100 GPa.

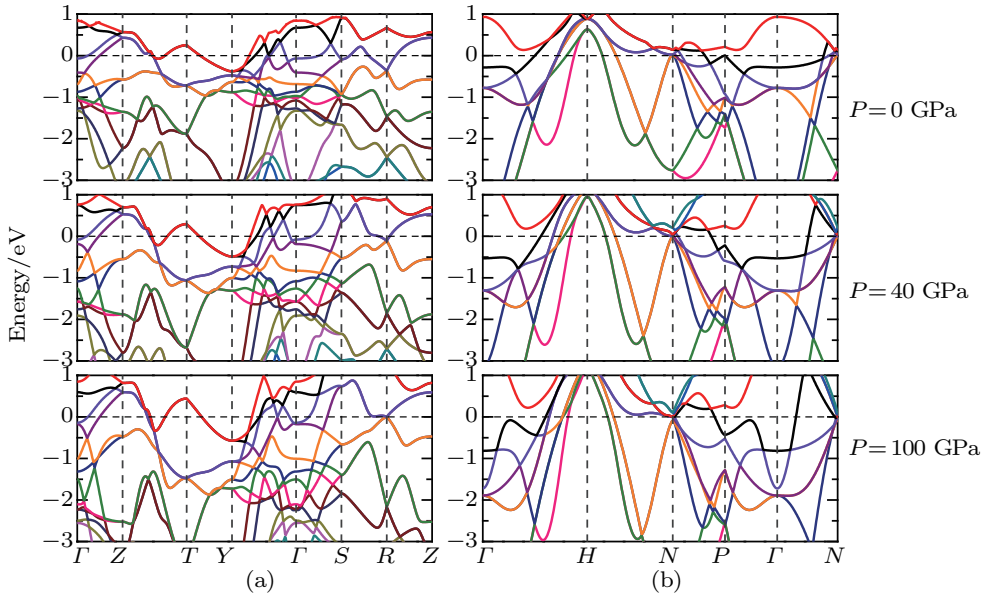


Fig. 5. (color online) The band structures at 0, 40, and 100 GPa for (a) α and (b) γ phases. The Fermi level is set at zero.

As shown in Fig. 5, a lot of bands cross the Fermi energy level in the Brillouin zone for both α and γ phases. Upon compression, this kind of crossing never changes visibly. This means that the conductivity of uranium should not vary too much under pressure.

3.3. Elastic properties

3.3.1. Elastic properties of α phase under high pressure

The elastic constants can measure the resistance and mechanical properties of a crystal under external stress, thus describing the stability of crystals against elastic deformation. We present the calculated elastic constants (C_{11}, C_{22}, C_{33}, C_{44}, C_{55}, C_{66}, C_{12}, C_{13}), Poisson's ratio (ν), elastic wave velocities (υ_t, υ_l, υ_m), and Debye temperature (θ_D) of α-U in Table 2. At 0 GPa, our results are comparable with previous pseudopotential calculations by Taylor *et al.*,[32] full-potential calculations by Soderlind *et al.*[16] as well as experiments at 298 K from Fisher and McSkimin.[45] The requirement of mechanical stability in an orthorhombic crystal lead to the following restriction on elastic constants[18]

$$\begin{aligned} &C_{ii}(i=1\sim6)>0,\\ &C_{11}+C_{22}+C_{33}+2(C_{12}+C_{13}+C_{23})>0,\\ &(C_{11}+C_{22}-2C_{12})>0,\\ &(C_{11}+C_{33}-2C_{13})>0,\\ &(C_{22}+C_{33}-2C_{23})>0. \end{aligned} \tag{8}$$

From the calculated values of C_{ij}, α-U is mechanical stable under pressure up to at least 100 GPa, which is consistent with that of experiments.[12–15] Besides, the nine elastic constants increase almost linearly from 0 GPa to 100 GPa.

Table 2. Calculated nine independent elastic constants (C_{11}, C_{22}, C_{33}, C_{44}, C_{55}, C_{66}, C_{12}, C_{13}, C_{23}), Poisson's ratio (ν), transverse (υ_t), longitudinal (υ_l), and average sound velocities (υ_m) derived from polycrystalline bulk and shear modulus, as well as Debye temperature (θ_D) of α phase at selected pressures.

Phase	C_{11}/GPa	C_{33}/GPa	C_{44}/GPa	C_{66}/GPa	C_{12}/GPa	C_{13}/GPa	B/GPa	G/GPa	E/GPa	ν	υ_t/(m/s)	υ_l/(m/s)	υ_m/(m/s)	θ_D/K
0	287.2	219.5	352.3	151.2	117.4	101.2	65.6	28.2	152.1	0.207	2337.6	3845.7	2582.6	282.7
20	459.3	339.6	527.5	204.6	182.1	145.7	102.6	56.8	210.5	0.211	2723.2	4497.1	3009.8	341.7
40	640.2	444.1	668.5	248.8	222.8	188.2	137.7	94.7	272.2	0.223	2962.1	4959.0	3278.3	381.1
60	801.7	534.6	795.3	283.8	254.9	230.1	176.4	124.2	339.0	0.234	3124.1	5301.4	3462.0	409.8
80	975.7	639.6	896.8	315.3	276.2	271.6	208.2	150.3	401.6	0.242	3265.5	5596.8	3622.0	435.2
100	1165.3	769.8	1020.4	355.2	293.3	310.2	223.7	167.0	452.9	0.242	3439.1	5894.7	3814.5	464.4
Calc.[32]	296	216	367	153	129	99	60	29	141	0.21				287
Calc.[16]	300	220	320	150	93	120	50	5	110	0.18				228
Expt.[45]	215	199	267	124	73	74	46	22	108	0.2				251

For the orthorhombic crystal system, the Voigt bulk modulus (B_V) and the Reuss bulk modulus (B_R) can be expressed by:

$$\begin{aligned} B_V &= (1/9)[C_{11}+C_{22}+C_{33}+2(C_{12}+C_{13}+C_{23})],\\ B_R &= \Delta[C_{11}(C_{22}+C_{33}-2C_{23})+C_{22}(C_{33}-2C_{13})\\ &\quad -2C_{33}C_{12}+C_{12}(2C_{23}-C_{12})+C_{13}(2C_{12}-C_{13})\\ &\quad +C_{23}(2C_{13}-C_{23})]^{-1},\\ \Delta &= C_{13}(C_{12}C_{23}-C_{13}C_{22})+C_{23}(C_{12}C_{13}-C_{23}C_{11})\\ &\quad +C_{33}(C_{11}C_{22}-C_{12}^2). \end{aligned} \tag{9}$$

The Voigt shear modulus (G_V) and the Reuss shear modulus (G_R) are defined as:

$$\begin{aligned} G_V &= (1/15)[C_{11}+C_{22}+C_{33}+3(C_{44}+C_{55}+C_{66})\\ &\quad -(C_{12}+C_{13}+C_{23})],\\ G_R &= 15\{4[C_{11}(C_{22}+C_{33}+C_{23})+C_{22}(C_{33}+C_{13})\\ &\quad +C_{33}C_{12}-C_{12}(C_{23}+C_{12})-C_{13}(C_{12}+C_{13})\\ &\quad -C_{23}(C_{13}+C_{23})]/\Delta+3[(1/C_{44})+(1/C_{55})\\ &\quad +(1/C_{66})]\}^{-1}. \end{aligned} \tag{10}$$

Their computational results are plotted in Fig. 6(a). By utilizing the VRH approximation,[41–43] B and G of α phase in pressure range of 0 GPa–100 GPa are plotted in Fig. 6(b). Here, the value of bulk modulus ($B = 147.5$ GPa) at ambient pressure turns out to be very close to the result from the EOS fitting (see Table 1). As is known to all that E is used to measure the stiffness of solids. The larger the value of Young's modulus becomes, the stiffer the material is. From present results of E, we can find that α phase is getting stiffer as the pressure increases. Furthermore, the bulk modulus represents the resistance to fracture, while the shear modulus can represent the resistance to plastic deformation. According to Pugh's[46] rule, if $B/G > 1.75$ (< 1.75), the material is ductile (brittle). The ratio of B/G is 1.37 for α, which indicates better performance of brittle elasticity at ambient pressure.

In addition, the effects of pressure on elastic moduli, elastic wave velocities, and Debye temperatures are evident. However, the Poisson's ratio is the most sluggish one upon compression. By using Eqs. (6) and (7), the average wave velocity and Debye temperature can be obtained. The value of Debye temperature is monotonically increasing. And the calculated value at 0 GPa is well consistent with recent theoretical result of 287 K[32] as well as the experimental result[45] of 251 K.

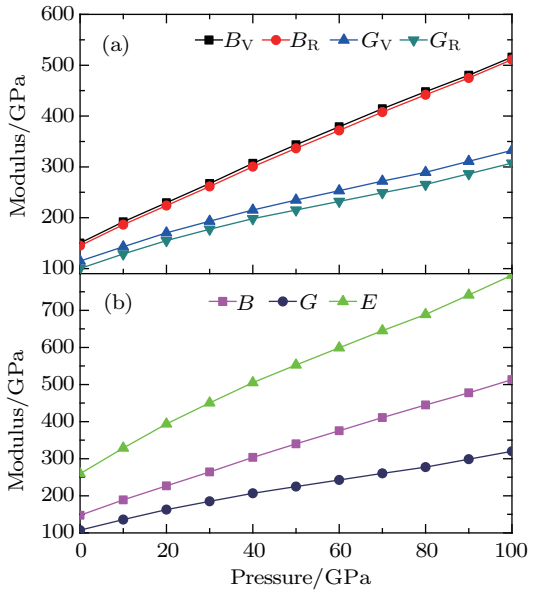


Fig. 6. (color online) Calculated bulk moduli B_V, B_R, B, shear moduli G_V, G_R, G, and Young's modulus E for α-U as a function of pressure. Solid lines are guides to the eyes.

It is very important to describe the elastic anisotropy behavior in engineering science and crystal physics. Crystal anisotropy reflects atomic arrangements along different directions. The shear anisotropic factors from our elastic constants are showed in Table 3. In the $\{100\}$ shear planes between the $\langle 011\rangle$ and $\langle 010\rangle$ directions is written as $A_1 = 4C_{44}/(C_{11}+C_{33}-2C_{13})$. For the $\{010\}$ shear planes between $\langle 101\rangle$ and $\langle 001\rangle$ directions, it is $A_2 = 4C_{55}/(C_{22}+C_{33}-2C_{23})$. And for the $\{001\}$ shear planes between $\langle 110\rangle$ and $\langle 010\rangle$ directions is defined as $A_3 = 4C_{66}/(C_{11}+C_{22}-2C_{12})$. For an isotropic crystal, the factors A_1, A_2, and A_3 must be one, while any value of them either smaller or greater than unity for orthorhombic structures. Our calculated results suggest that the shear anisotropic factor for the $\{010\}$ shear planes between $\langle 101\rangle$ and $\langle 001\rangle$ directions show more anisotropic than the other two shear planes upon compression.

Table 3. The anisotropic factors for α and β phases.

Phase	Pressure/GPa	A_1	A_2	A_3
α	0	1.037	1.753	1.078
	20	0.937	1.633	0.981
	40	0.889	1.569	0.931
	60	0.842	1.564	0.934
	80	0.842	1.564	0.936
	100	0.767	1.326	0.834
β	0	1.198	1.019	0.701

3.3.2. Elastic properties of β and γ phases at ambient condition

For β-U and γ-U, we list their elastic constants, elastic moduli, elastic wave velocities, and Debey temperature in Table 4, in comparison with other theoretical results.[28,29,32,47] Here, the B_V, B_R, G_V, and G_R of tetragonal and cubic structures are derived by the following formula:[40]

$$\begin{aligned} B_V &= (1/9)[2(C_{11}+C_{12})+4C_{13}+C_{33}], \\ B_R &= C^2/M, \\ M &= C_{11}+C_{12}+2C_{33}-4C_{13}, \\ C^2 &= (C_{11}+C_{12})C_{33}-2C_{13}^2, \\ G_V &= (1/30)(M+3C_{11}-3C_{12}+12C_{44}+6C_{66}), \\ G_R &= 15\{(18B_V/C^2)+[6/(C_{11}-C_{12})]+(6/C_{44}) \\ &\quad +(3/C_{66})\}^{-1}, \end{aligned} \tag{11}$$

and

$$\begin{aligned} B_V &= B_R = (C_{11}+2C_{12})/3, \\ G_V &= (C_{11}-C_{12}+3C_{44})/5, \\ G_R &= 5(C_{11}-C_{12})C_{44}/[4C_{44}+3(C_{11}-C_{12})], \end{aligned} \tag{12}$$

respectively. Our calculated elastic constants for β-U are well consistent with the values from Li *et al.*[28] It is mechanically stable in the ground state because elastic constants satisfy the following mechanically stable criteria[40] of tetragonal structure:

$$\begin{aligned} &C_{11} > 0, \quad C_{11}-C_{12} > 0, \quad C_{33} > 0, \\ &C_{44} > 0, \quad [2(C_{11}-C_{12})+C_{33}+4C_{13}] > 0, \\ &C_{66} > 0, \quad (C_{11}+C_{33}-2C_{13}) > 0. \end{aligned} \tag{13}$$

In fact, the C_{12} of β-U is much smaller than C_{11}, the value of B, G, E, and θ_D decrease from the α phase to the β phase. The obtained bulk modulus value turns out to be accord with the result from the EOS fitting (see Table 1) at ambient pressure. Besides, the ratio of B/G ($\sim$2.4) is above 1.75, which illustrates that tetragonal structure is ductile.

Furthermore, there are three elastic anisotropic factors in the tetragonal systems defined as $A_1 = 2C_{66}/(C_{11}-C_{12})$, $A_2 = 4C_{44}/(C_{11}+C_{33}-2C_{13})$, and $A_3 = C_{44}/C_{66}$. The shear anisotropic factors A_1 represents the $\{001\}$ shear planes while the elastic anisotropic factors A_2 for the $\{0\bar{1}1\}$ shear planes along the $\langle 011\rangle$ direction. The A_3 anisotropy relation corresponds to the shear along the $\langle 010\rangle$ and $\langle 100\rangle$ directions in the $\{001\}$ and $\{010\}$ planes, and their values are listed in Table 3. It is noted that anisotropy relation corresponds to the shear along the $\langle 010\rangle$ and $\langle 100\rangle$ directions in the $\{001\}$ and $\{010\}$ planes are more important than the other two shear planes.

Elastic constants unsatisfy the mechanically stable criteria[40] of cubic structure, so the γ phase is mechanically unstable

$$\begin{aligned} &C_{11} > 0, \quad C_{44} > 0, \\ &C_{11} > |C_{12}|, \quad (C_{11}+2C_{12}) > 0. \end{aligned} \tag{14}$$

The calculations show that C_{11} is much smaller than C_{12}, which is agreement with other theoretical calculations.[29,32,47]

Table 4. Elastic constants of the β and γ phases of uranium, bulk modulus (B), shear modulus (G), Young's modulus (E), Poisson's ratio (ν), transverse (υ_t), longitudinal (υ_l), and average sound velocities (υ_m) derived from polycrystalline properties, as well as Debye temperature (θ_D) at 0 K.

Phase	C_{11}/GPa	C_{33}/GPa	C_{44}/GPa	C_{66}/GPa	C_{12}/GPa	C_{13}/GPa	B/GPa	G/GPa	E/GPa	ν	υ_t/(m/s)	υ_l/(m/s)	υ_m/(m/s)	θ_D/K
β	219.9	212.6	45.3	64.6	111.9	77.0	131.1	54.6	146.4	0.314	1704.9	3273.9	1907.7	207.0
Calc.[29]	220	201	65	36	94	79	130	85	210	0.23				253
Calc.[28]	218	214	60	61	99	80	130							
γ	71.8		41.7		165.5		134.2	88.6	217.9	0.229	2128.4	3592.0	2357.3	257.6
Calc.[29]	86		37		155		132	113	265	0.17				289
Calc.[32]	161		56		184		176							
Calc.[47]	84		38		159		133	102	243	0.2				274

For bulk modulus, shear modulus, Young's modulus, Poisson's ratio, transverse, longitudinal, average sound velocities, as well as Debey temperature of γ are listed in Table 4. These results are compared with the values from Taylor[32] and Shang[47] who employed the PW91-GGA exchange-correlation functional. Moreover, the value of the bulk modulus (B = 113 GPa) slightly overestimates experimental calculation by Yoo *et al.*[13] The ratio of B/G ($\sim$1.5) of γ phase demonstrates that bcc structure uranium is brittle in ground state.

4. Conclusion

In summary, the structural, electronic, and mechanical properties of the α, β, and γ phases of uranium under pressure up to 100 GPa have been studied by employing the first-principles DFT-GGA method. Our calculations show that the lowest energy structure of U is α-phase (orthorhombic *Cmcm*-type). By calculating the enthalpies of the three phases, we never find any phase transitions in pressure range of 0 GPa–100 GPa. According to our calculated elastic constants, α and β phases are mechanically stable at ambient pressure. For γ phase, however, it is mechanically unstable at 0 GPa. Under pressure, the bulk modulus B, shear modulus G, and Young's modulus E increase near linearly for α phase.

References

[1] Prodan I D, Scuseria G E and Martin R L 2007 *Phys. Rev. B* **76** 033101
[2] Atta Fynn R and Ray A K 2007 *Phys. Rev. B* **76** 115101
[3] Zhang P, Wang B T and Zhao X G 2010 *Phys. Rev. B* **82** 144110
[4] Wang B T, Zhang P, Lizárraga R, Marco I D and Eriksson O 2013 *Phys. Rev. B* **88** 104107
[5] Ao B Y, Shi P, Guo Y and Gao T 2013 *Chin. Phys. B* **22** 037103
[6] Yang R, Tang B, Gao T and Ao B Y 2016 *Chin. Phys. B* **25** 067106
[7] Wang B T and Zhang P 2011 *Chin. Phys. Lett.* **28** 047101
[8] Li L, Wang B T and Zhang P 2015 *Chin. Phys. Lett.* **32** 037102
[9] Pfleiderer C 2009 *Rev. Mod. Phys.* **81** 1551
[10] Santini P, Carretta S, Amoretti G, Caciuffo R, Magnani N and Lander G H 2009 *Rev. Mod. Phys.* **81** 807
[11] Zhang X, Zhang H, Wang J, Felser C and Zhang S C 2012 *Science* **335** 1464
[12] Akella J, Smith G S, Grover R, Wu Y and Martin S 1990 *High Press. Res.* **2** 295
[13] Yoo C S, Cynn H, and Söderlind P 1998 *Phys. Rev. B* **57** 10359
[14] Le Bihan T, Heathman S, Idiri M, Lander G H, Wills J M, Lawson A C and Lindbaum A 2003 *Phys. Rev. B* **67** 134102
[15] Dewaele A, Bouchet J, Occelli F, Hanfland M and Garbarino G 2013 *Phys. Rev. B* **88** 134202
[16] Söderlind P 2002 *Phys. Rev. B* **66** 085113
[17] Richard N, Bernard S, Jollet S and Torrent M 2002 *Phys. Rev. B* **66** 235112
[18] Yang J W, Gao T, Liu B Q, Sun G A and Chen B 2014 *Eur. Phys. J. B* **87** 130
[19] Lawson A, Olsen C, Richardson J, Mueller M and Lander G 1988 *Acta Cryst. B* **44** 89
[20] Wang B T, Zhang P, Liu H Y, Li W D and Zhang P 2011 *J. Appl. Phys.* **109** 063514
[21] Souvatzis P, Eriksson O, Katsnelson M I and Rudin S P 2008 *Phys. Rev. Lett.* **100** 095901
[22] Söderlind P, Eriksson O, Johansson B, Wills J M and Boring A M 1995 *Nature* **374** 524
[23] Söderlind P, Grabowski B, Yang L and Landa A 2012 *Phys. Rev. B* **85** 060301
[24] Fisher E S and McSkimin H G 1961 *Phys. Rev.* **124** 67
[25] Crummett W P, Smith H G, Nicklow R M and Wakabayashi N 1979 *Phys. Rev. B* **19** 6028
[26] Manley M E, Lander G H, Sinn H, Alatas A, Hults W L, McQueeney R J, Smith J L and Willit J 2003 *Phys. Rev. B* **67** 052302
[27] Barrett C S, Mueller M H and Hitterman R L 1963 *Phys. Rev. B* **129** 625
[28] Li J H, Chen Q B, Lu C H, Lu L, Dai Y and Liu B X 2012 *J. Alloys Compd.* **516** 139
[29] Beeler B, Deo C, Baskes M and Okuniewski M 2013 *J. Nucl. Mater.* **433** 143
[30] Beeler B, Deo C, Baskes M and Okuniewski M 2012 *J. Phys.: Condens. Matter.* **24** 075401
[31] Chen Q Y, Tan S Y, Lai X C and Chen J 2012 *Chin. Phys. B* **21** 087801
[32] Taylor C 2008 *Phys. Rev. B* **77** 094119
[33] Bouchet J 2008 *Phys. Rev. B* **77** 024113
[34] Fast L, Eriksson O, Johansson B, Wills J, Straub G, Roeder H and Nordstrom L 1998 *Phys. Rev. Lett.* **81** 2978
[35] Raymond S, Bouchet J, Lander G H, Tacon M L, Garbarino G, Hoesh M, Rueff J P, Krisch M, Lashley J C, Schulze R K and Albers R C 2011 *Phys. Rev. Lett.* **107** 136401
[36] Qiu R Z, Lu H Y, Ao B Y, Tang T and Chen P H 2016 *Modelling Simul. Mater. Sci. Eng.* **24** 055011
[37] Kresse G and Furthmuller J 1996 *Phys. Rev. B* **54** 11169
[38] Perdew J P, Burke K and Ernzerhof M 1996 *Phys. Rev. Lett.* **77** 3865
[39] Monkhorst H J and Pack J D 1972 *Phys. Rev. B* **13** 5188
[40] Nye J F 1985 *Physical Properties of Crystals* (Oxford: Clarendon Press) p. 135
[41] Voigt W 1928 *Lehrburch der Kristallphysik* (Leipzig: Teubner Verlag Leipzig) p. 739
[42] Reuss A and Angew Z 1929 *Math. Mech.* **9** 49
[43] Hill R 1952 *Proc. Phys. Soc.* **65** 349
[44] Wilson A and Rundle R 1949 *Acta Cryst.* **21** 26
[45] Fisher E and McSkimin H 1958 *J. Appl. Phys.* **29** 1473
[46] Pugh S F 1954 *Philos. Mag.* **45** 823
[47] Shang S, Saengdeejing A, Mei Z, Kim D, Zhang H, Ganeshan S, Wang Y and Liu Z 2010 *Comp. Mater. Sci.* **48** 813